



Structural feature controlling superconductivity in compressed BaFe₂As₂

Wenge Yang, Feng-Jiang Jia, Ling-Yun Tang, Qian Tao, Zhu-An Xu, and Xiao-Jia Chen

Citation: *Journal of Applied Physics* **115**, 083915 (2014); doi: 10.1063/1.4867159

View online: <http://dx.doi.org/10.1063/1.4867159>

View Table of Contents: <http://scitation.aip.org/content/aip/journal/jap/115/8?ver=pdfcov>

Published by the [AIP Publishing](#)



Re-register for Table of Content Alerts

Create a profile.



Sign up today!



Structural feature controlling superconductivity in compressed BaFe₂As₂

Wenge Yang,^{1,2,a)} Feng-Jiang Jia,³ Ling-Yun Tang,^{1,4} Qian Tao,⁵ Zhu-An Xu,⁵
and Xiao-Jia Chen^{1,3,6,b)}

¹Center for High Pressure Science and Technology Advanced Research, Shanghai 201203, China

²High Pressure Synergetic Consortium, Geophysical Laboratory, Carnegie Institution of Washington, Argonne, Illinois 60439, USA

³Key Laboratory of Materials Physics and Center for Energy Matter in Extreme Environments, Institute of Solid State Physics, Chinese Academy of Sciences, Hefei 230031, China

⁴Department of Physics, South China University of Technology, Guangzhou 510640, China

⁵Department of Physics, Zhejiang University, Hangzhou 310027, China

⁶Geophysical Laboratory, Carnegie Institution of Washington, Washington, DC 20015, USA

(Received 7 November 2013; accepted 17 February 2014; published online 28 February 2014)

Superconductivity can be induced with the application of pressure but it disappears eventually upon heavy compression in the iron-based parent compound BaFe₂As₂. Structural evolution with pressure is used to understand this behavior. By performing synchrotron X-ray powder diffraction measurements with diamond anvil cells up to 26.1 GPa, we find an anomalous behavior of the lattice parameter with a *S* shape along the *a* axis but a monotonic decrease in the *c*-axis lattice parameter with increasing pressure. The close relationship between the axial ratio *c/a* and the superconducting transition temperature *T_c* is established for this parent compound. The *c/a* ratio is suggested to be a measure of the spin fluctuation strength. The reduction of *T_c* with the further increase of pressure is a result of the pressure-driven weakness of the spin-fluctuation strength in this material. © 2014 AIP Publishing LLC. [<http://dx.doi.org/10.1063/1.4867159>]

I. INTRODUCTION

The discovery of superconductivity in the electron-doped LaFeAsO system¹ at a transition temperature *T_c* of 26 K ushered a new wave of high temperature superconductors after 20 yr of discovery of cuprites. Similar to the Cu-O layer in cuprates, the structure feature of the conduction Fe-As layer sandwiched by insulating layers plays the key role in superconductivity in this new type of iron-based family. After that, many iron-based superconductors have been found. Up to now, there are mainly six types of iron-based superconductors, such as 1111-type LnFeAsO (Ln = La, Sm, Ce, Pr, Nd, etc.),^{1,2} 122-type AFe₂As₂ (A = Ba, Sr, Ca, and Eu),³ 111-type BFeAs (B = Li, Na, and K),⁴ 11-type FeSe(Te),⁵ 21311-type Sr₂ScO₃FeX (X = P and As),⁶ and 122*-type C_{0.8}Fe_{2-y}Se₂ (C = K, Rb, and Cs).⁷ Among these families, 122-type compound AFe₂As₂ (A = Ba, Sr, Ca, and Eu) can be easily synthesized to high purity single crystal, thus it is an ideal system to study the fundamental physical properties under various conditions (pressure, temperature, external magnetic fields, etc.). The 122-type compound exhibits a magnetic and structural phase transition upon cooling before superconducting phase emerging, while strong anomalies in the specific heat, electrical resistivity, and magnetic susceptibility occur at this transition.^{8–10} At ambient pressure, the BaFe₂As₂ compound⁸ has the magnetic and structural phase transition at temperature about 140 K. The hole or electron doping usually suppresses the long-range structural and antiferromagnetic ordering, which can lead to the emergence of superconductivity at low temperature. For instance,

K-doped compound Ba_{1-x}K_xFe₂As₂ reaches a maximum *T_c* of 38 K,¹¹ Co-doped compound BaFe_{2-x}Co_xAs₂ shows a *T_c* of 22 K with *x* = 0.2,¹² and Ni-doped BaFe_{2-x}Ni_xAs₂ also exhibits a *T_c* of 20.5 K with *x* = 0.1.¹³

Pressure as one of the fundamental state parameters can be used to tune the lattice and electronic structure efficiently, which alters the structural and magnetic ordering. Recent neutron scattering measurements on the parent compound BaFe₂As₂ revealed that modest strain fields along the in-plane orthorhombic *b* axis can affect significant the structural and magnetic phase transitions.¹⁴ This system does not show superconducting properties at ambient pressure and low temperature even at liquid helium temperature (~4 K) without doping, but *T_c* reaches 29 K at the applied pressure of 4 GPa.¹⁵ Many high-pressure investigations have been performed in different kinds of iron-based compounds to understand the pressure and doping effects on superconductivity.¹⁶ However, the detailed interplay between structural instabilities and superconductivity has not been fully understood due to the lack of information on the pressure dependence of the structural properties.

Extensive investigations on the parent compound BaFe₂As₂^{17–19} have showed that BaFe₂As₂ undergoes a phase transition from a tetragonal (T) to a collapsed tetragonal (CT) phase at 27 GPa at room temperature, while it transforms from an orthorhombic phase to a tetragonal phase at 33 K at 29 GPa. For the sister system CaFe₂As₂, the transitional pressure value is about 2 GPa at room temperature, which is much smaller than that of BaFe₂As₂. Jorgensen *et al.*¹⁸ reported that the structural transition for BaFe₂As₂ at room temperature is from a tetragonal to orthorhombic phase at 17 GPa. Meanwhile, density functional theory calculation¹⁹ shows that BaFe₂As₂ has a transition from a magnetic

^{a)}Electronic mail: wyang@ciw.edu

^{b)}Electronic mail: xjchen@ciw.edu

orthorhombic phase to a collapsed tetragonal phase through an intermediate nonmagnetic tetragonal phase at low temperature. In contrast, CaFe_2As_2 transforms from a magnetic orthorhombic phase to a nonmagnetic collapsed tetragonal phase at 3 GPa or 0.48 GPa for hydrostatic or uniaxial pressure at low temperature. Therefore, the structural evolution of 122-type iron-based compounds is not yet well understood.

In this work, we report a systematic structural study of BaFe_2As_2 at the pressures up to 26.1 GPa using the synchrotron X-ray diffraction technique. We found that the lattice parameters a and c decrease monotonically at pressure range from ambient to 10.1 GPa. Then the structure exhibits an abnormal compression behavior, the lattice parameter a first increases continuously and reaches maximum at 21.0 GPa while maximum a value even surpasses the ambient condition lattice constant a and then decreases rapidly till 26.1 GPa, the highest pressure in this study; but the lattice parameter c decreases monotonically with increasing pressure in the entire range of our measurements. Comparing the transition temperatures reported in literatures on this system at the studied pressure range,^{15,20–25} we correlate the internal relationship between the axial ratio c/a and the T_c reported in the literatures: Superconductivity can only occur in a certain range of axial ratio, and the maximum T_c under pressure is largely related to the deviation of this ratio from the optimal value.

II. EXPERIMENTAL DETAILS

Single crystal sample BaFe_2As_2 was grown by the self-flux method with the high-purity elements Ba, Fe using FeAs as the flux, detailed procedures of synthesizing the samples have been reported somewhere else.¹³ For getting good powder diffraction data, one piece of single crystal was crashed and grounded carefully to make fine powder grains without large strain.

Powder diffraction was carried out with the angle-dispersive X-ray diffraction experiments at beamline 16BM-D, HPCAT, the Advanced Photon Source of the Argonne National Laboratory. The incident monochromatic beams were focused to 5–10 μm (FWHM) with wavelength of 0.38745 Å. The experimental parameters were calibrated with NIST standard CeO_2 powder diffraction. A symmetric diamond anvil cell with a pair of 400 μm culet size anvils was used to generate high pressure. A stainless steel gasket preindented to 35 μm thick with a 180 μm diameter hole was used as the sample chamber. A small piece of sample pallet with a ruby ball was loaded in the gasket hole. Silicone oil was used as pressure transmission medium to maintain quasi-hydrostatic pressure environment in the studied pressure range. The pressures were monitored by the ruby fluorescence shifts. A mar345 image plate was used to collect the powder diffraction patterns. The 2d diffraction data were integrated using FIT2D²⁶ and analyzed by the Rietveld refinement with the FULLPROF program.²⁷

III. RESULTS AND DISCUSSION

Figure 1 shows the angle-dispersive powder x-ray diffraction patterns of BaFe_2As_2 at various pressures and room temperature. Below 11.8 GPa, the diffraction peaks in all angle range remain relatively unchanged but shift to high two theta angle

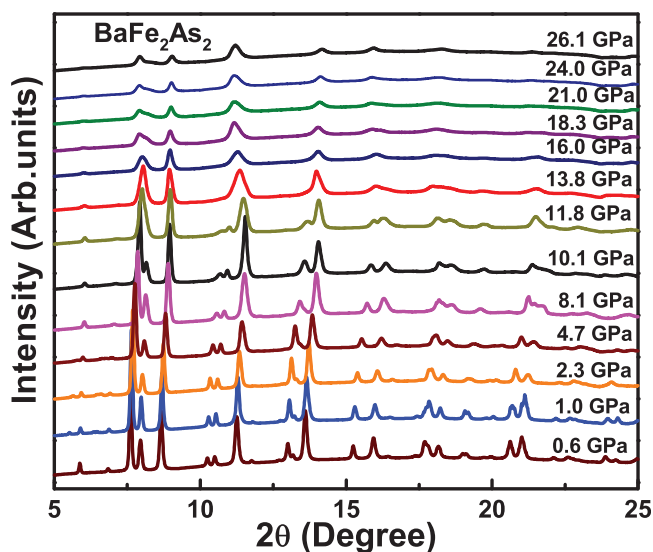


FIG. 1. The integrated powder diffraction patterns of BaFe_2As_2 at various pressures and room temperature.

sides, indicating regular compression behavior. At 11.8 GPa, the original two peaks between 7.5° and 8.5° combine into one. Upon a further increase of pressure, the diffraction peaks become wider and the intensity of peaks becomes weaker. Above 11.8 GPa, the two peaks between 10° and 12.5° become a single peak and this single peak shifts to the lower angle side, which is clear evidence of the corresponding lattice expanding while pressure increasing. Beyond 21 GPa, the powder patterns look similar. This indicates that the new phase completes the transition and follows a normal compression behavior.

In order to retrieve crystal structure and precise lattice parameters, we have conducted Rietveld refinements on all these power X-ray diffraction data, considering the peak broadening effect in the high-pressure range. All peaks can be indexed well with a tetragonal structure (space group $I4/mmm$) up to 26.1 GPa. Figure 2 shows a Rietveld refine of

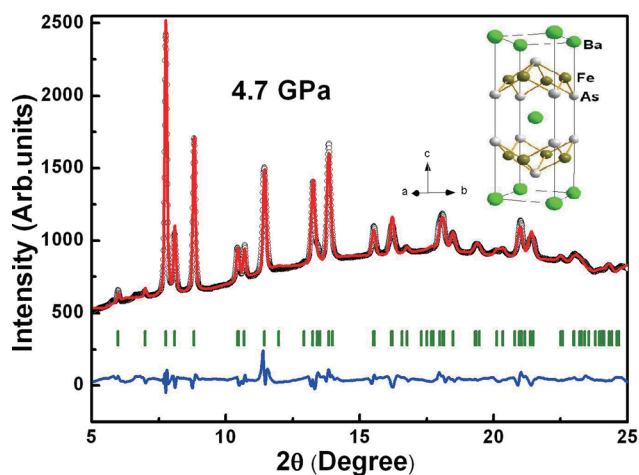


FIG. 2. Observed (solid black circle), calculated (continuous red line), difference between observed and calculated (bottom blue line), and the positions of the Bragg reflections (vertical green lines) profiles obtained after Rietveld refinements of X-ray diffraction patterns of BaFe_2As_2 using tetragonal space group ($I4/mmm$) at 4.7 GPa and room temperature. The inset shows the crystal structure of BaFe_2As_2 with tetragonal ThCr_2Si_2 -type at 4.7 GPa and room temperature.

BaFe₂As₂ at a pressure of 4.7 GPa. The difference between the observed and the calculated X-ray diffraction intensity distribution is quite reasonable. When we try to fit the higher pressure structure with other possible structure such as orthorhombic *Fmmm* phase, which is reported previously,¹⁸ the fit results are quite poor. The inset shows the crystal structure of BaFe₂As₂ with ThCr₂Si₂-type at 4.7 GPa and room temperature. Comparing to the structure of BaFe₂As₂ at ambient pressure, the lattice parameters decrease about 2%.

Figure 3 shows the pressure dependence of the lattice parameters *a* and *c* of BaFe₂As₂ at room temperature obtained from Rietveld refinement for entire pressure range. The lattice parameters *a* and *c* shrink in pressure from ambient to 10.1 GPa. Upon further compression, the structure exhibits an abnormal behavior: the lattice parameter *a* first increases, and reaches maximum at 21.0 GPa, then decreases to the maximum pressure studied in this investigation; while the lattice parameter *c* decreases with pressure in the entire range of our measurements. We noticed that the structural transition from a tetragonal to a collapsed tetragonal phase completes at above 21 GPa, and both phases have the space group *I4/mmm*. Below 11.8 GPa, the refinement results give high precision lattice parameters (error bar is less than 0.1%, which is smaller than the size of symbol); above 11.8 GPa, peak broadening and reduced peak intensity cause the fitting results a little larger uncertainty (about 0.1%–0.2%, on the size of the symbol in the plot of *a* and *c* vs. pressure), which can be seen from the measured values slightly deviated from the fitted curve. But nevertheless, this does not change our main results.

Figure 4 shows the pressure dependence of the axial ratio *c/a* and the *T_c* reported from various groups. The *c/a* ratio shows a gradual decrease with increasing pressure till 10.1 GPa and then follows a rapid decrease in pressure range from 10.1 GPa to 21.0 GPa. Above 21.0 GPa, the ratio *c/a* is nearly a constant. The results for *T_c* vs pressure are obtained from various groups^{15,20–25} and summarized in Table I. The pressure-transmitting medium (“Medium”), the maximum pressure (“*P_{max}*”) with superconducting phase, the maximum

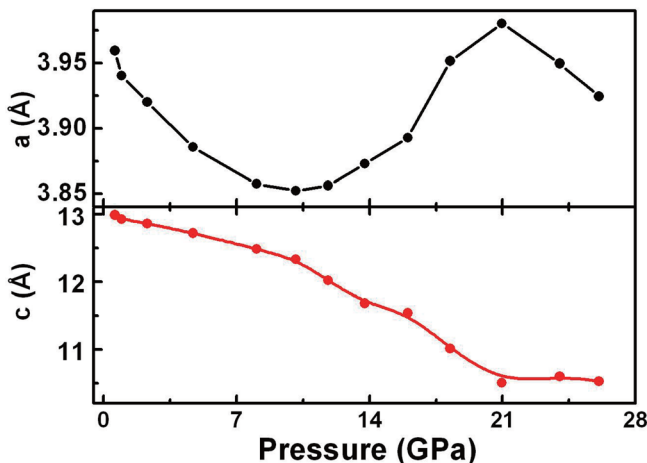


FIG. 3. Pressure dependence of the lattice parameters *a* and *c* of BaFe₂As₂ at room temperature obtained after Rietveld refinement of data with increasing pressure.

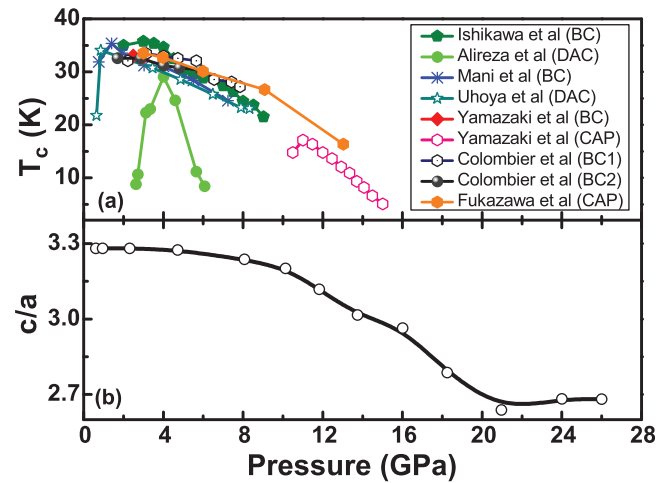


FIG. 4. Pressure dependence of the superconducting transition temperature *T_c* and the axial ratio *c/a* for BaFe₂As₂.

superconducting transition temperature (“Max *T_c*”) and the corresponding critical pressure (“*P_c*”) are also listed in Table I.

Figure 5 shows the unit cell volume *V* as a function of pressure in the parent compound BaFe₂As₂ at room temperature, where the red lines are the fitting results by using the third-order Birch-Murnaghan equation of state,²⁸

$$P = \frac{3}{2}B_0 \left[\left(\frac{V}{V_0} \right)^{-7/3} - \left(\frac{V}{V_0} \right)^{-5/3} \right] \times \left\{ 1 + \frac{3}{4}(B'_0 - 4) \left[\left(\frac{V}{V_0} \right)^{-2/3} - 1 \right] \right\}, \quad (1)$$

where *B₀* is the bulk modulus, *B'₀* the derivative of bulk modulus at ambient pressure, and *V₀* the volume at ambient pressure. With *B'₀* being fixed as 4.0, we have *B₀* = 54.9 ± 2.0 Å³ and *V₀* = 203.1 ± 0.9 Å³. These results are comparable to those for the tetragonal phase of electron-doped compound BaFe_{1.8}Ni_{0.2}As₂²⁹ and those reported earlier for the parent compound.¹⁷

The experimental and theoretical results^{17,30} show that the Fe-Fe and Fe-As bond lengths reveal anomaly increase

TABLE I. Summary of pressure studies on the parent compound BaFe₂As₂. The pressure “Technique” of Bridgman cell (BC), cubic-anvil press (CAP), and diamond anvil cell (DAC), in association with a specific pressure “Medium” are listed. Maximum superconducting transition temperatures (“Max *T_c*” in K units) at the critical pressure (“*P_c*” in GPa units), the Maximum pressure (“*P_{max}*” in GPa units) are also listed. None indicates no pressure transmission medium was used.

Technique	Medium	Max <i>T_c</i> (<i>P_c</i>)	<i>P_{max}</i>	Ref.
BC	FC 70/77	35 (3)	9	20
DAC	Daphne oil 7373	29 (4)	6	15
BC	Steatite	35 (1.5)	7.2	22
DAC	None	34 (1)	8.3	21
BC	FC 70/77	33 (3)	3	23
CAP	Daphne oil 7474	17 (11.5)	16	23
BC1	FC 70/77	30 (5.5)	8	24
BC2	FC 70/77	31 (4.7)	5.7	24
CAP	FC 70/77	25 (3)	13	25

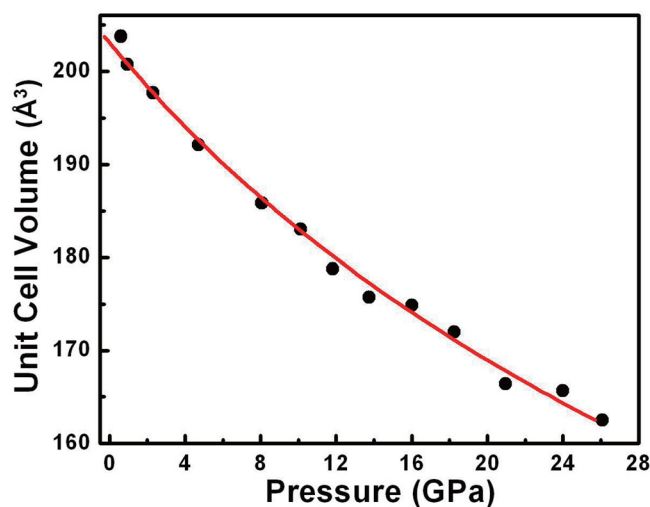


FIG. 5. Pressure dependence of the unit cell volume V of BaFe_2As_2 . The red line represents a fit to the third-order Birch-Murnaghan equation as described in the text.

with increasing pressure and this anomaly was associated with loss of magnetism. The loss of magnetism may increase the As-As interaction along the c axis. Conversely, this would change the parameter z of the As atom and may lead to an increase in the distortion of the As-Fe-As bond angle. This indicates that the magnetism is a crucial factor controlling the lattice parameters in the parent compound BaFe_2As_2 .

Up to now, the temperature dependence of the electrical resistivity measurements of the parent compound BaFe_2As_2 at different pressures was carried out by various groups using the Bridgman cell (BC), the cubic-anvil press (CAP), and the diamond anvil cell (DAC).^{15,20–25} Duncan *et al.*³¹ found that the pressure-temperature phase diagrams of BaFe_2As_2 were different because of the different pressure environment, which was provided by the different cells and the different pressure-transmitting media. As mentioned earlier, we used Silicone oil as pressure transmitting medium, as it provides the quasi-hydrostatic condition for the entire pressure range studied. The structure transformation from the tetragonal to collapsed tetragonal phase occurs at 21.0 GPa, which is much lower than that reported previously,¹⁷ where the Helium was used as pressure transmitting medium to maintain the best hydrostatic condition. In other words, the hydrostatic pressure increases considerably the critical phase transition pressure for the parent compound BaFe_2As_2 . This result indicates that the phase transition is sensitive to uniaxial stress of pressure as observed by neutron measurements.¹⁴

The iron-based compound BaFe_2As_2 composes of alternating Ba layer and FeAs layer. In this, strongly correlated electron system, the superconductivity occurs when the magnetostructural order is completely suppressed by electron doping or the application of pressure, etc. However, the applied pressure has very little effect on superconductivity in the optimally electron-doped $\text{BaFe}_{1.8}\text{Co}_{0.2}\text{As}_2$ compared to the underdoped $\text{BaFe}_{1.92}\text{Co}_{0.08}\text{As}_2$.¹² As for parent BaFe_2As_2 compound, external pressure is needed to tune the lattice and electronic structure to suppress the magnetic ordering and induce the superconductivity. The bond angle As-Fe-As and bond length Fe-As are the key components for

the structure evolution related to superconductivity. The highest T_c values are found when the As-Fe-As tetrahedral bond angle is close to the ideal value of 109.47° , which can be used as a guide to explore the possible higher T_c superconductor by electron doping and/or pressure. In this investigation, Rietveld refinements on the powder diffraction data at the studied pressure range provide the atomic positions of all Ba, Fe, and As, which are reflected in the lattice parameters and space group symmetry. Thus, the lattice change can be treated as a sensor of the changes of Fe-As bond length and As-Fe-As bond angle, which directly reflects the distance between layers. Therefore, there is an optimized c/a ratio to maintain the As-Fe-As tetrahedral bond angle close to the ideal value of 109.47° for superconductivity. For the present compound BaFe_2As_2 , the c/a decreases gradually below 10 GPa following by a rapid decrease in the pressure range from 10 to 21 GPa before reaching a much lower constant. As a result, T_c of BaFe_2As_2 may be highest at 4 GPa and then it could decrease with increasing pressure. At 21 GPa and above, the ratio c/a is too far for the structure to maintain the superconducting phase.

Band structure calculations^{32–35} show that the suppression of the antiferromagnetic state and the emergence of superconductivity can be attributed to nesting between electron and hole Fermi surface sheets. Increasing pressure results in the reduction of the axial ratio c/a to increase inter-plane hopping and warp the original cylinder-like Fermi surface sheets. As a result, the nesting between electron and hole Fermi surface sheets is reduced. This effect may suppress the spin density wave order and induce superconductivity. These theoretical works demonstrate that the axial ratio c/a should be related to the superconductivity.

According to the relationship between the pressure and the T_c shown in Figure 4 and the information in Table I, we can conclude that the transition pressure for the T to CT phase transition is relatively low (21 GPa comparing to 28 GPa) with hydrostatic pressure transmitting medium, the maximum T_c is about 35 K with critical pressure ~ 4 GPa, and the pressure ranges where superconductivity appears differ among research groups. Alireza *et al.*¹⁵ reported that T_c reaches a maximum at about 4 GPa using a miniature diamond anvil cell. They used single-crystalline samples and Daphne 7373 as a pressure-transmitting medium. Ishikawa *et al.*²⁰ reported that the maximum T_c is about 35 K, where the pressure is about 3 GPa, and the Fluorinert 70 and 77 were used as the pressure-transmitting medium. Uhoya *et al.*,²¹ Mani *et al.*,²² Yamazaki *et al.*,²³ Colombier *et al.*,²⁴ and Fukazawa *et al.*²⁵ also reported the pressure dependence of T_c but their results are different. Therefore, the transport property measurements at higher pressures are still necessary for the clarification. In Figure 4, the behavior of axial ratio c/a is nicely related to the T_c behavior reported by Fukazawa *et al.*²⁵ These authors²⁵ used a cubic anvil apparatus at pressure values of up to 13 GPa with a 1:1 mixture of Fluorinerts 70 and 77. In their experiments, T_c reaches a maximum at about 3 GPa. When pressure is beyond 3 GPa, T_c decreases. This offers another evidence of the relationship between the axial ratio c/a and superconductivity.

The close relationship between the ratio c/a and superconductivity demonstrates that the three-dimensional feature of the structure in BaFe_2As_2 is in favor of superconductivity. This finding supports the three-dimensional nature of the superconducting gap and its sensitivity to the antiferromagnetic ordering wave vectors Q along the c axis.^{36,37} Once the parent compound becomes superconducting at high pressures, the reduction of the three-dimensional structural feature would weaken the superconducting behavior and eventually destroys superconductivity. This picture is consistent with the well established relation between the neutron spin resonance energies at $Q = (0.5, 0.5, 0)$ and $(0.5, 0.5, 1)$ and T_c in $\text{BaFe}_{2-x}\text{B}_x\text{As}_2$ ($B = \text{Ni, Co}$).³⁷ In the neutron measurements, Wang *et al.*³⁷ found that the anisotropic spin gaps at the two wave vectors $Q = (0.5, 0.5, 0)$ and $(0.5, 0.5, 1)$ decrease with increasing electron-doping. By doping more electrons, T_c decreases in the overdoped region and the over spin excitations gradually transform into quasi-two-dimensional spin excitations. Thus, our finding not only follows that the axial ratio c/a is indeed a measure of spin fluctuation but also offers evidence for the spin-fluctuation-mediated superconductivity in these iron arsenide compounds. Indeed, a close correlation between the spin fluctuations and superconductivity under pressure was recently observed in an Iron-based superconductor.³⁸

IV. CONCLUSIONS

We have investigated the high-pressure behaviors of the undoped parent compound BaFe_2As_2 at room temperature through the high-pressure powder synchrotron X-ray diffraction technique. The intrinsic relationship between the axial ratio c/a and the superconductivity in this parent has been established. We found that the lattice parameter a exhibits an anomalous behavior upon compression with a S shape while the lattice parameter c decreases monotonically with pressure. We proposed that the c/a ratio is a measure of the spin fluctuation strength. The pressure-driven weakness of the spin-fluctuation strength accounts for the observed reduction of T_c with the applied pressure in the parent 122 compound.

ACKNOWLEDGMENTS

X-ray diffraction measurements were supported as part of Energy Frontier Research in Extreme Environments Center (EFree), an Energy Frontier Research Center funded by the U.S. Department of Energy, Office of Science, Office of Basic Energy Sciences under Award No. DE-SG0001057. Sample synthesis and data analysis in China were supported by the Cultivation Fund of the Key Scientific and Technical Innovation Project Ministry of Education of China (No. 708070), the National Basic Research Program of China (Grant No. 2011CBA00103), the National Natural Science Foundation of China (Nos. 10874046 and 11174247), Guangdong Natural Science Foundation (No. S2012040007929), and the Fundamental Research Funds for the Central Universities SCUT (No. D213235w). The use of HPCAT, APS is supported by Carnegie Institute of Washington, Carnegie DOE Alliance Center, University of Nevada at Las Vegas, and Lawrence

Livermore National Laboratory through funding from DOE-National Nuclear Security Administration, DOE-Basic Energy Sciences, and NSF. APS was supported by DOE-BES, under Contract No. DE-AC02-06CH11357.

- ¹Y. Kamihara, T. Watanabe, M. Hirano, and H. Hosono, *J. Am. Chem. Soc.* **130**, 3296 (2008).
- ²Z. A. Ren, W. Lu, J. Yang, W. Yi, X. L. Shen, Z. C. Li, G. C. Che, X. L. Dong, L. L. Sun, F. Zhou, and Z. X. Zhao, *Chin. Phys. Lett.* **25**, 2215 (2008).
- ³M. Rotter, M. Tegel, and D. Johrendt, *Phys. Rev. Lett.* **101**, 107006 (2008).
- ⁴X. C. Wang, Q. Q. Liu, Y. X. Lv, W. B. Gao, L. X. Yang, R. C. Yu, F. Y. Li, and C. Q. Jin, *Solid State Commun.* **148**, 538 (2008).
- ⁵F. C. Hsu, J. Y. Luo, K. W. Yeh, T. K. Chen, T. W. Huang, P. M. Wu, Y. C. Lee, Y. L. Huang, Y. Y. Chu, D. C. Yan, and M. K. Wu, *Proc. Natl. Acad. Sci. U. S. A.* **105**, 14262 (2008).
- ⁶I. R. Shein and A. L. Ivanovskii, *Phys. Rev. B* **79**, 245115 (2009).
- ⁷J. G. Guo, S. F. Jin, G. Wang, S. C. Wang, K. X. Zhu, T. T. Zhou, M. He, and X. L. Chen, *Phys. Rev. B* **82**, 180520(R) (2010).
- ⁸M. Rotter, M. Tegel, and D. Johrendt, *Phys. Rev. B* **78**, 020503(R) (2008).
- ⁹F. Ronning, T. Klimczuk, E. D. Bauer, H. Volz, and J. D. Thompson, *J. Phys.: Condens. Matter* **20**, 322201 (2008).
- ¹⁰M. Tegel, M. Rotter, V. Weiss, F. M. Schappacher, R. Poettgen, and D. Johrendt, *J. Phys.: Condens. Matter* **20**, 452201 (2008).
- ¹¹N. Ni, S. L. Bud'ko, A. Kreyssig, S. Nandi, G. E. Rustan, A. I. Goldman, S. Gupta, J. D. Corbett, A. Kracher, and P. C. Canfield, *Phys. Rev. B* **78**, 014507 (2008).
- ¹²K. Ahilan, J. Balasubramanian, F. L. Ning, T. Imai, A. S. Sefat, R. Jin, M. A. McGuire, B. C. Sales, and D. Mandrus, *J. Phys.: Condens. Matter* **20**, 472201 (2008).
- ¹³L. J. Li, Y. K. Luo, Q. B. Wang, H. Chen, Z. Ren, Q. Tao, Y. K. Li, X. Lin, M. He, Z. W. Zhu, G. H. Cao, and Z. A. Xu, *New J. Phys.* **11**, 025008 (2009).
- ¹⁴C. Dhital, Z. Yamanni, W. Tian, J. Zeretsky, A. S. Sefat, Z. Q. Wang, R. J. Birgeneau, and S. D. Wilson, *Phys. Rev. Lett.* **108**, 087001 (2012).
- ¹⁵P. L. Alireza, Y. T. Chris Ko, J. Gillett, C. M. Petrone, J. M. Cole, G. G. Lonzarich, and S. E. Sebastian, *J. Phys.: Condens. Matter* **21**, 012208 (2009).
- ¹⁶C. W. Chu and B. Lorenz, *Physica C* **469**, 385 (2009).
- ¹⁷R. Mittal, S. K. Mishra, S. L. Chaplot, S. V. Ovsyannikov, E. Greenberg, D. M. Trots, L. Dubronvinsky, Y. Su, T. Brueckel, S. Matsuishi, H. Hosono, and G. Garbarino, *Phys. Rev. B* **83**, 054503 (2011).
- ¹⁸J. E. Jørgensen, J. S. Olsen, and L. Gerward, *Solid State Commun.* **149**, 1161 (2009).
- ¹⁹M. Tomić, R. Valentí, and H. O. Jeschke, *Phys. Rev. B* **85**, 094105 (2012).
- ²⁰F. Ishikawa, N. Eguchi, M. Kodama, K. Fujimaki, M. Einaga, A. Ohmura, A. Nakayama, A. Mitsuda, and Y. Yamada, *Phys. Rev. B* **79**, 172506 (2009).
- ²¹W. Uhoya, A. Stemshorn, G. Tsoi, Y. K. Vohra, A. S. Sefat, B. C. Sales, K. M. Hope, and S. T. Weir, *Phys. Rev. B* **82**, 144118 (2010).
- ²²A. Mani, N. Ghosh, S. Paulraj, A. Bharathi, and C. S. Sundar, *Europhys. Lett.* **87**, 17004 (2009).
- ²³T. Yamazaki, N. Takeshita, R. Kobayashi, H. Fukazawa, Y. Kohori, K. Kihou, C. H. Lee, H. Kito, A. Iyo, and H. Eisaki, *Phys. Rev. B* **81**, 224511 (2010).
- ²⁴E. Colombier, S. L. Bud'ko, N. Ni, and P. C. Canfield, *Phys. Rev. B* **79**, 224518 (2009).
- ²⁵H. Fukazawa, N. Takeshita, T. Yamazaki, K. Kondo, K. Hirayama, Y. Kohori, K. Miyazawa, H. Kito, H. Eisaki, and A. Iyo, *J. Phys. Soc. Jpn.* **77**, 105004 (2008).
- ²⁶A. P. Hammersley, S. O. Svensson, M. Hanfland, A. N. Fitch, and D. Hausermann, *High Pressure Res.* **14**, 235 (1996).
- ²⁷J. Rodríguez-Carvajal, *Physica B* **192**, 55 (1993).
- ²⁸F. Birch, *Phys. Rev.* **71**, 809 (1947).
- ²⁹F. J. Jia, W. G. Yang, L. J. Li, Z. A. Xu, and X. J. Chen, *Physica C* **474**, 1 (2012).
- ³⁰H. Okada, K. Igawa, H. Takahashi, Y. Kamihara, M. Hirano, H. Hosono, K. Matsubayashi, and Y. Uwatoko, *J. Phys. Soc. Jpn.* **77**, 113712 (2008).
- ³¹W. J. Duncan, O. P. Welzel, C. Harrison, X. F. Wang, X. H. Chen, F. M. Grosche, and P. G. Niklowitz, *J. Phys.: Condens. Matter* **22**, 052201 (2010).

- ³²S. A. J. Kimber, A. Kreyssig, Y. Z. Zhang, H. Jeschke, R. Valenti, F. Yokaichiya, E. Colombier, J. Yan, T. C. Hansen, T. Chatterji, R. J. McQueeney, P. C. Canfeld, A. I. Goldman, and D. N. Argyriou, *Nature Mater.* **8**, 471 (2009).
- ³³D. J. Singh, *Phys. Rev. B* **78**, 094511 (2008).
- ³⁴I. R. Shein and A. L. Ivanovskii, *J. Exp. Theor. Phys. Lett.* **88**, 107 (2008).
- ³⁵Y. Z. Zhang, H. C. Kandpal, I. Opahle, H. O. Jeschke, and R. Valenti, *Phys. Rev. B* **80**, 094530 (2009).
- ³⁶S. X. Chi, A. Schneidewind, J. Zhao, L. W. Harriger, L. J. Li, Y. K. Luo, G. H. Cao, Z. A. Xu, M. Loewenhaupt, J. P. Hu, and P. C. Dai, *Phys. Rev. Lett.* **102**, 107006 (2009).
- ³⁷M. Y. Wang, H. Q. Luo, J. Zhao, C. L. Zhang, M. Wang, K. Marty, S. X. Chi, J. W. Yynn, A. Schneidewind, S. L. Li, and P. C. Dai, *Phys. Rev. B* **81**, 174524 (2010).
- ³⁸G. F. Ji, J. S. Zhang, L. Ma, P. Fan, P. S. Wang, J. Dai, G. T. Tan, Y. Song, C. L. Zhang, P. C. Dai, B. Normand, and W. Q. Yu, *Phys. Rev. Lett.* **111**, 107004 (2013).